

Comparative current–voltage characteristics of nicked and repaired λ -DNA

B. Hartzell and B. McCord

Nanoscale and Quantum Phenomena Institute, and Department of Chemistry and Biochemistry, Ohio University, Athens, Ohio 45701

D. Asare, H. Chen, J. J. Heremans, and V. Soghomonian^{a)}

Nanoscale and Quantum Phenomena Institute, and Department of Physics and Astronomy, Ohio University, Athens, Ohio 45701

(Received 6 January 2003; accepted 1 May 2003)

We report on current–voltage characteristics obtained at room temperature on λ -DNA molecules, modified at both ends with disulfide groups and spanning Au electrodes. A comparison is drawn between the characteristics of the λ -DNA, which after modification features a gap between 3' and 5' sites (nicked DNA), and λ -DNA where this gap has been ligated (repaired DNA). The repaired DNA double helices show a close-to-linear current–voltage characteristic, and a dc conductivity estimated at $\sim 1 \times 10^{-3} \text{ S cm}^{-1}$. In contrast, the nicked DNA shows pronouncedly nonlinear and rectifying behavior, with a conductivity gap of $\sim 3 \text{ eV}$. The low-field conductivity of the nicked DNA is approximately a factor 20 lower than the repaired DNA's conductivity. © 2003 American Institute of Physics. [DOI: 10.1063/1.1588738]

The structure of DNA, with its wire-like double helix, and π -electron-rich stacked base pairs, has led to considerable interest in the molecule's electronic properties. The interest in charge transport through DNA is driven both by biological considerations, involving radiation damage and repair,¹ as well as by the molecule's potential use as molecular wire in nanoelectronics. Initial measurements concerned photoinduced charge transfer,² whereas recent studies have focused on direct electrical conductivity measurements. Yet, the electrical conductivity measurements have yielded a conflicting range of both experimental and theoretical results, ascribing to the molecule a wide range of conductivities, as well as variably indicating the presence or absence of an activation gap.^{3,4} Presently, an explanation is emerging that attributes the wide scatter in the data to the ease with which DNA can be modified and with which it conforms to various environments. The experiments are typically performed in a variety of conditions where important factors, including the surface of the substrate, contacts to the electrodes, DNA sequence, counterions, and DNA secondary structure (bends, nicks, stacking distance between base pairs, width of the DNA molecule), are not kept constant. Here we report on direct electrical conductivity measurements on λ -DNA under conditions that yield reproducible results, and we analyze the role of unrepaired nicks in a double stranded DNA molecule introduced during disulfide linker attachment.

The specimens used in our study were λ -DNA molecules functionalized with disulfide groups at their 3' ends, synthesized using the hybridization method of Braun *et al.* with minor adaptations.⁵ The $16 \mu\text{m}$ long, linear viral λ -DNA was obtained from Sigma-Aldrich. In its linear form λ -DNA possesses, at both ends, two short overhang regions 12 bases long. These overhang regions were utilized in the following procedure to functionalize both ends of λ -DNA with disulfide groups, allowing attachment to Au electrodes for con-

ductivity measurements. Single strands of 12 base length from Integrated DNA Technologies, labeled with C3 S–S disulfide groups at their 3' ends, were used. These single strand sequences were complementary to the 12 unpaired bases of each overhang region, and were hybridized to these regions of λ -DNA, effectively providing a complete, double stranded molecule with a gap in each strand. That is, gaps existed between the 5' ends of the complementary single strands and the 3' ends of the λ -DNA substrate, resulting in nicked DNA molecules (Fig. 1). Our experiments compare the current–voltage characteristics obtained on nicked λ -DNA to identical λ -DNA samples with the nicks repaired by ligation. The repaired DNA was prepared by first removing the 5' phosphate groups on both ends of the λ -DNA using shrimp alkaline phosphatase to prevent circularization of λ -DNA during ligation. The two 12 base single strands were phosphorylated using T4 polynucleotide kinase (MBI

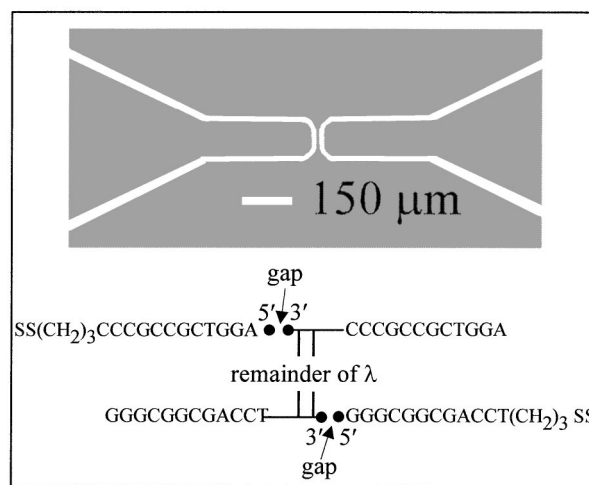


FIG. 1. Below: sketch of the disulfide-labeled λ -DNA molecules used in this work. The nicked DNA features a gap between the 3' and 5' nucleotides, where indicated. In the repaired DNA, the gaps were repaired using T4 DNA ligase. Above: the Au electrode geometry, on Si/SiO₂ substrates.

^{a)}Electronic mail: soghomon@ohio.edu

Fermentas) and one of these oligonucleotides was hybridized to λ by cooling slowly from 75 °C. The nick in the phosphate backbone between this oligonucleotide and λ was then repaired using T4 ligase (MBI Fermentas). The mixture was filtered to remove excess free oligonucleotide and then the second oligonucleotide was hybridized and ligated to λ in the same manner. To verify that the earlier-mentioned enzymatic manipulations worked properly, one of the 12 base complementary oligonucleotides was labeled with a fluorescent dye. After completion of the final ligation step, the λ -DNA sample was cleaved with a restriction enzyme (*Bgl*III, New England BioLabs) to yield smaller fragments that could be analyzed by denaturing capillary electrophoresis coupled with laser induced fluorescence detection. As expected, a single-strand, fluorescent fragment, with a length greater than the 12 base complementary oligonucleotide, was detected (fragment of 419 base length), confirming the realization of successful enzymatic ligations.

Electrodes were fabricated using standard lithography techniques, on *p*-type doped Si (100) substrates capped with 4500 Å thermal oxide. The metal stack consisted of a 80 Å Cr sticking layer, followed by a 300 Å Au layer, evaporated after photolithography. A lift-off procedure resulted in the electrode geometry depicted in Fig. 1. The electrodes are separated by 8 μm , and run parallel over a length of 50 μm . The quarter-circle opening of the electrode gap toward the electrical contacts was provided to avoid electric field concentrations. After lithography the samples were boiled in acetone to remove traces of photoresist, then cleaned in a heated ammonium hydroxide/hydrogen peroxide mixture to remove organic residues, and finally were again boiled in acetone and subsequently in methylene chloride. This rigorous cleaning procedure of the electrodes prior to DNA attachment proved necessary to obtain reproducible results, presumably because the procedure leads to abundant Au sites, facilitating the formation of a chemisorbed disulfide-Au bond, and hence, adequate electrical contacts.⁶ We also noticed that photoresist profiles leaving an upturned edge to the electrodes led to poor results, demonstrating the need to control the fabrication procedure.

Manipulation by ac electric fields was used to orient the DNA strands between the two electrodes, by applying a field of strength 10^6 V/m at a frequency of 1 MHz over the electrodes.^{7,8} The success of this method of alignment was visually confirmed using confocal microscopy and a DNA fluorescent intercalating dye. In our procedure, the ac field was applied to the device and subsequently a 2 μL drop of the appropriate DNA solution (1–5 nM) was centered over the electrodes. During the 25 min alignment the sample was kept within a hydration chamber where the relative humidity was maintained between 85% and 90% to control droplet evaporation. After removing the ac field, the device was left for an additional 25 min in the chamber to allow for sufficient Au–S bond formation. The long alignment time and bond formation time, under controlled humidity, were necessary to obtain repeatable trapping of the DNA and, hence, consistent electrical contacts. The alignment was followed by a rinse with de-ionized water to remove both unbound DNA and buffer solution. The sample was then dried under a flow of nitrogen gas. A similar procedure using a dc electric field

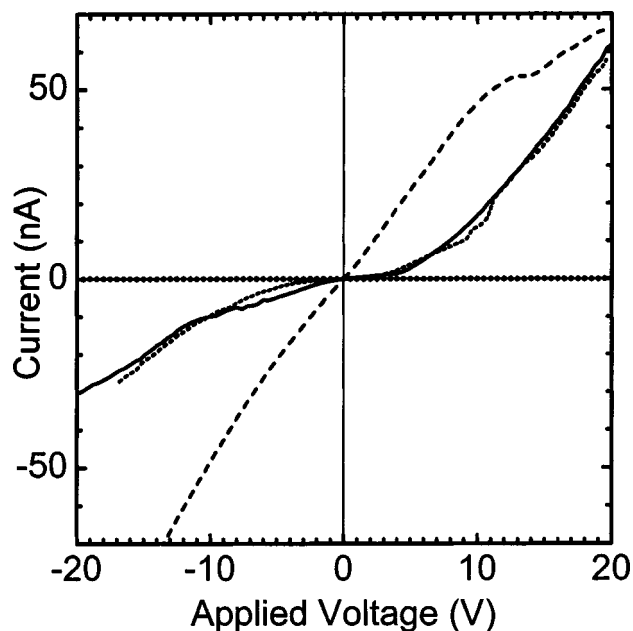


FIG. 2. Current–voltage characteristics measured at room temperature on disulfide-labeled λ -DNA molecules. Dashes: repaired DNA; dots: nicked DNA, swept from negative to positive potential; solid line: nicked DNA, swept from positive potential to negative potential; filled circles: electrodes without DNA (zero line).

of 10^6 V/m proved less reliable. To quantify parasitic conductance resulting from traces of buffer or ligase solution and salt bridges, a base line measurement was performed on a tenfold excess solution of buffer and ligase. In a procedure identical to that for depositing DNA solution, a droplet of the buffer and ligase was placed onto a device, and dried under a flow of nitrogen gas. The maximum value of the current, in the range from -20 to 20 V, was measured to be 1 nA. In contrast, the open electrode measurements yielded on the order of 2 pA, and actual DNA devices yielded several tens of nanoamperes. Hence, in our procedure, we may neglect parasitic conductance channels in all but the most detailed measurements.

I – V characteristics were measured on the samples under ambient condition and at room temperature. A slight dependence on humidity was noticed, and forms the subject of further study, but will be neglected in the present work. Figure 2 compares I – V characteristics obtained on nicked λ -DNA, to characteristics obtained on repaired λ -DNA. The figure also shows the current measured before DNA deposition, as a zero line. For the nicked λ -DNA, the I – V characteristic is pronouncedly nonlinear, showing a conductivity gap up to $\sim \pm 3$ V, beyond which sizable current flow occurs. Voltage sweeps were performed both in the negative to positive direction and reverse, and the fine structure as well as the overall shape of the data is mirrored around zero bias for up compared to down sweeps. The individual I – V curves are slightly asymmetric around zero bias, and fine structure appears around 7–12 V bias (positive bias for up sweep, negative bias for down sweep). The up and down voltage sweeps are expected to mirror each other if source and drain electrodes hold interchangeable roles. Although the DNA molecule is not precisely symmetric around its mid point, in this case the close-to-random potential landscape provided by the long base sequences ($\sim 24\,000$ bases long) between the

source and drain electrodes restores the source-to-drain device interchangeability. In our experiments, the up and down sweeps differ slightly due to the mirroring described earlier. A strong hysteresis in $I-V$ curves is an indication of conductivity through residual salt bridges.⁹ But, since in our experiments the up and down sweeps mirror each other closely, since we do not observe a dependence on the bias sweep rate, and since we previously quantified the contribution of salt bridges, we believe salt bridges do not contribute significantly to the $I-V$ characteristics of our devices when prepared by the described procedures (deviations from these procedures indeed result in significant and time-dependent hysteresis attributable to salt bridges).

The repaired λ -DNA showed a significantly more ohmic behavior, with no observable conductivity gap when the same potential sweeps were applied. The current values between the curves cannot unambiguously be compared, since the number of DNA strands captured and measured for different devices can vary, due to uncertainties in the trapping procedure and in the electrical contact formation. Yet, since reproducible $I-V$ curves could be obtained for both repeated measurements on the same DNA sample and measurements on different electrode devices, we believe using our method $I-V$ curve shapes can be compared, as can order of magnitude estimates of DNA conductivity. Assuming one layer of DNA makes electrical contact with the electrodes, the repaired DNA in Fig. 2 shows a low-field dc electrical conductivity of $\sim 3 \times 10^{-3} \text{ S cm}^{-1}$. This value should be regarded as an upper bound, given the measurement uncertainties, involving the number of strands, the two-contact geometry utilized, the nature of electrical contacts and others. Different samples conserve the $I-V$ curve shape, but show dc conductivities ranging from $6 \times 10^{-4} \text{ S cm}^{-1}$ to $3 \times 10^{-3} \text{ S cm}^{-1}$. Such values fall around the literature average^{3,4,10-15} and are below conductivities of well-studied undoped conductive polymers such as polyacetylene ($\sim 10^{-2} \text{ S cm}^{-1}$).¹⁶

The low-field ($< 3 \text{ V}$) dc conductivity of the nicked DNA is reduced by a factor ~ 20 compared to the repaired DNA. We estimate that the two unrepaired 3-5' gaps introduce an additional low-field resistance of $\sim 100 \text{ T } \Omega$ per double helical DNA strand. At higher fields, the 3-5' gaps introduce a rectification effect, as can be appreciated from the asymmetric $I-V$ characteristics. Since little current is flowing before the onset of conduction at $\sim 3 \text{ V}$ bias, we assume most of this potential drop falls over the gap region, and deduce that a threshold energy of $\sim 3 \text{ eV}$ is necessary for carriers to overcome the 3-5' gaps. Whether the voltage threshold is due to the presence of an energy barrier, due to interband tunneling or due to a Coulomb blockade effect is uncertain at this point. However, the 3 eV value lies in the range of energies mentioned in the theoretical and experimental literature.^{10,17} Interestingly, each of the gaps falls over one strand of the

double helix (Fig. 1). The gapless complementary strand apparently does not shunt the current, indicating that the complete double helical structure plays an important role in electronic transport. This finding is consistent with recent reports of much decreased conductivity in single stranded DNA.^{10,18} The features in the $I-V$ characteristic at $\pm 10 \text{ V}$ are only observed in nicked DNA, and hence also must be attributed to the 3-5' gap. At $\sim +13 \text{ V}$, a small plateau develops in the $I-V$ for the repaired DNA. This plateau appears independently of sweep direction in disulfide-labeled repaired DNA, always at high positive bias. A detailed understanding of the excitations and energy levels giving rise to these features has not yet been achieved.

In conclusion, we have developed a reproducible method for the measurement of $I-V$ characteristics on λ -DNA and have applied the method toward a comparison of electronic transport through nicked and repaired DNA molecules. The repaired DNA shows a close-to-linear $I-V$ characteristic, whereas the nicked DNA shows a conductivity threshold. The different $I-V$ characteristics point to the promise of electronic functionalization of DNA, by exploiting the molecule's versatile and well-studied chemistry. Moreover, selective modification of DNA molecules and their subsequent electronic characterization can lead to a better understanding of DNA's electronic transport properties.

The authors acknowledge support from the National Science Foundation (NIRT No. 0103034).

¹B. Giese, *Annu. Rev. Biochem.* **71**, 51 (2002).

²S. O. Kelley and J. K. Barton, *Science* **283**, 375 (2002).

³D. Porath, A. Bezryadin, S. de Vries, and C. Dekker, *Nature (London)* **403**, 635 (2000).

⁴H. Fink and C. Schönberger, *Nature (London)* **398**, 407 (1999).

⁵E. Braun, Y. Eichen, U. Sivan, and G. Ben-Yoseph, *Nature (London)* **391**, 775 (1998).

⁶K. W. Hipps, *Science* **294**, 536 (2001).

⁷M. Washizu and O. Kurosawa, *IEEE Trans. Ind. Appl.* **26**, 1165 (1990).

⁸A. Bezryadin, C. Dekker, and G. Schmid, *Appl. Phys. Lett.* **71**, 1273 (1997).

⁹Y. Zhang, R. H. Austin, J. Kraeft, E. C. Cox, and N. P. Ong, *Phys. Rev. Lett.* **89**, 198102 (2002).

¹⁰Y. Okahata, T. Kobayashi, H. Nakayama, and K. Tanaka, *Supramol. Sci.* **5**, 317 (1998).

¹¹A. J. Storm, J. van Noort, S. de Vries, and C. Dekker, *Appl. Phys. Lett.* **79**, 3881 (2001).

¹²K. H. Yoo, J. O. Lee, J. W. Park, J. Kim, H. Y. Lee, T. Kawai, and H. Y. Choi, *Phys. Rev. Lett.* **87**, 198102 (2001).

¹³A. Y. Kasumov, M. Kociak, S. Guéron, B. Reulet, V. T. Volkov, D. V. Klinov, and H. Bouchiat, *Science* **291**, 280 (2001).

¹⁴P. J. de Pablo, F. Moreno-Herrero, J. Colchero, J. Gómez Herrero, P. Herrero, A. M. Baró, P. Ordejón, J. M. Soler, and E. Artacho, *Phys. Rev. Lett.* **85**, 4992 (2000).

¹⁵P. Tran, B. Alavi, and G. Gruner, *Phys. Rev. Lett.* **85**, 1564 (2000).

¹⁶T. A. Skotheim, *Handbook of Conductive Polymers* (Marcel Dekker, New York, 1986).

¹⁷M. Hjort and S. Stafstrom, *Phys. Rev. Lett.* **87**, 228101 (2001).

¹⁸V. Soghomonian (unpublished).